

Origin of the optical phonon frequency shifts in ZnO quantum dots

Khan A. Alim, Vladimir A. Fonoberov, and Alexander A. Balandin^{a)}

Nano-Device Laboratory, Department of Electrical Engineering, University of California–Riverside, Riverside, California 92521

(Received 8 November 2004; accepted 7 December 2004; published online 25 January 2005)

We carried out nonresonant and resonant Raman spectroscopy of ZnO quantum dots with diameter of 20 nm. On the basis of our measurements and comparison with a recently developed theory, we were able to clarify the origin of the observed phonon peak shifts in quantum dots as compared to bulk ZnO. It has been found that the spatial confinement of optical phonons in 20-nm-diameter dots leads to only few cm^{-1} peak shifts. At the same time, we have demonstrated, that even a low-power ultraviolet laser excitation, required for the resonant Raman spectroscopy of ZnO, leads to strong local heating of the ZnO quantum dots, which results in very large ($\sim 14 \text{ cm}^{-1}$) redshifts of the optical phonon peaks. We have estimated from the observed redshift that the local temperature of the quantum dot ensemble is about 700 °C. The obtained results are important for identification of phonon peaks in the Raman spectra of ZnO nanostructures. © 2005 American Institute of Physics. [DOI: 10.1063/1.1861509]

Nanostructures made of zinc oxide (ZnO), a wide-band-gap semiconductor, have recently attracted a lot of attention due to their proposed applications in low-voltage and short-wavelength (368 nm) electro-optical devices, transparent ultraviolet (UV) protection films, and gas sensors. Both resonant and nonresonant Raman scattering spectra have been measured for ZnO nanostructures such as thin films,^{1,2} nanowires,^{3,4} nanotubes,⁵ and nanoparticles.^{6–8} Due to the wurtzite crystal structure of bulk ZnO, the frequencies of both longitudinal optical (LO) and transverse optical (TO) phonons are split into two frequencies with symmetries A_1 and E_1 . In ZnO, in addition to LO and TO phonon modes, there are two nonpolar Raman active phonon modes with symmetry E_2 . The low-frequency E_2 mode is associated with the vibration of the heavy Zn sublattice, while the high frequency E_2 mode involves only the oxygen atoms. The above phonon modes are clearly identified in the Raman scattering spectra of bulk ZnO.^{9,10} The Raman spectra of ZnO nanostructures always show shift of the bulk phonon frequencies.^{1–8} The origin of this shift, its strength, and dependence on the quantum dot (QD) diameter are still the subjects of debates. Understanding the nature of the observed shift is important for interpretation of the Raman spectra and understanding properties of ZnO nanostructures.

In this letter, we present data that clarify the origin of the peak shift. There are three main mechanisms that can induce phonon peak shifts in ZnO nanostructures: (i) spatial confinement within the dot boundaries; (ii) phonon localization by defects (oxygen deficiency, zinc excess, surface impurities, etc.); or (iii) laser-induced heating in nanostructure ensembles. Usually, only the first mechanism, referred to as optical phonon confinement, is invoked as an explanation of the phonon frequency shifts in ZnO nanostructures.⁶

The optical phonon confinement has been originally introduced to explain the observed frequency shift in small covalent semiconductor nanocrystals. It attributes the redshift and broadening of the Raman peaks to the relaxation of the phonon wave vector selection rule due to the finite size of

the nanocrystals.¹¹ It has been recently shown theoretically¹² that while this phenomenological model is justified for small covalent nanocrystals, it cannot be applied to ionic ZnO QDs with the sizes larger than 4 nm. The latter is due to the fact that the polar optical phonons in ZnO are almost nondispersive in the region of small wave vectors. In addition, the asymmetry of the wurtzite crystal lattice leads to the QD shape-dependent splitting of the frequencies of polar optical phonons in a series of discrete frequencies. Here, we argue that all three aforementioned mechanisms contribute to the observed peak shift in ZnO nanostructures, and that in many cases, the contribution of the optical phonon confinement can be relatively small compared to other mechanisms.

We carried out systematic nonresonant and resonant Raman spectroscopy of ZnO QDs with diameter of 20 nm together with the bulk reference sample. To elucidate the effects of heating we varied the excitation laser power over a wide range. The reference wurtzite bulk ZnO crystal (University Wafers) had dimensions $5 \times 5 \times 0.5 \text{ mm}^3$ with a -plane (11–20) facet. The investigated ZnO QDs have been produced by the wet chemistry method. The dots had nearly spherical shape of the average diameter of 20 nm, and good crystalline structure as evidenced by the TEM study. The purity of ZnO QDs in a powder form was 99.5%. A Ren-

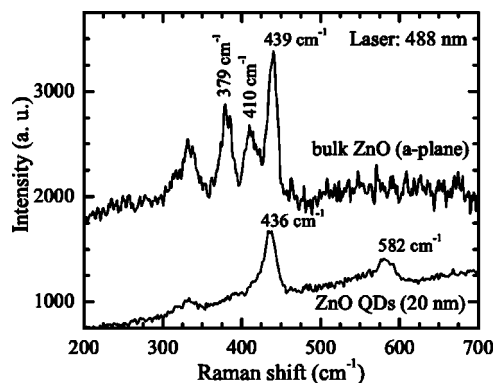


FIG. 1. Nonresonant Raman scattering spectra of bulk ZnO (a -plane) and ZnO quantum dots (20 nm in diameter). Laser power is 15 mW. Linear background is subtracted for the bulk ZnO spectrum.

^{a)}Electronic mail: alexb@ee.ucr.edu

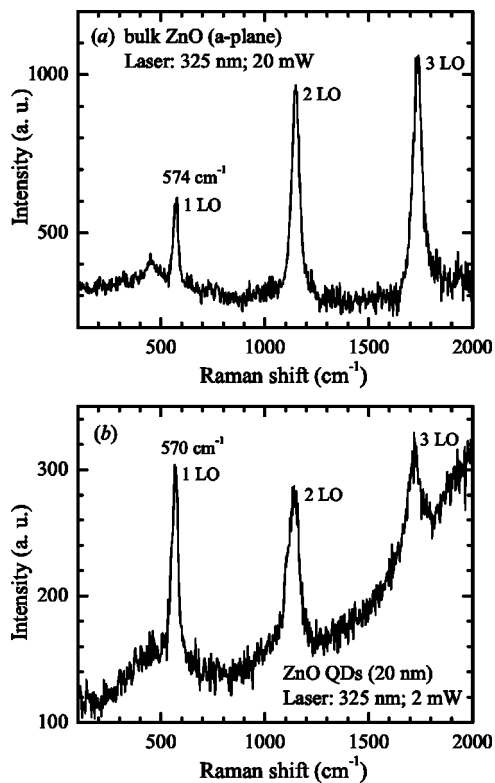


FIG. 2. Resonant Raman scattering spectra of (a) *a*-plane bulk ZnO and (b) ZnO quantum dots. Laser power is 20 mW for bulk ZnO and 2 mW for ZnO quantum dots. Photoluminescence background is subtracted from the bulk ZnO spectrum.

ishaw micro-Raman spectrometer 2000 with visible (488 nm) and UV (325 nm) excitation lasers was employed to measure the nonresonant and resonant Raman spectra of ZnO, correspondingly. The number of gratings in the Raman spectrometer was 1800 for visible laser and 3000 for UV laser. All spectra were taken in the backscattering configuration.

The obtained nonresonant and resonant Raman spectra of bulk ZnO crystal and ZnO QD sample are shown in Figs. 1 and 2, respectively. For comparison, a compilation of the reported frequencies of Raman active phonon modes in bulk ZnO is presented in Table I. In our spectrum from the bulk ZnO, the peak at 439 cm^{-1} corresponds to E_2 (high) phonon, while the peaks at 410 and 379 cm^{-1} correspond to E_1 (TO) and A_1 (TO) phonons, correspondingly. No LO phonon peaks are seen in the spectrum of bulk ZnO. On the contrary, no TO phonon peaks are seen in the Raman spectrum of ZnO QDs. In the QD spectrum, the LO phonon peak at 582 cm^{-1} has a frequency intermediate between those of A_1 (LO) and E_1 (LO) phonons (see Table I), which is in agreement with theoretical calculations.¹² The broad peak at about 330 cm^{-1} seen in both spectra in Fig. 1 is attributed to the second-order Raman processes.

TABLE I. Frequencies (in units of cm^{-1}) of Raman active phonon modes in bulk ZnO. Presented data are a compilation of the results of different studies listed in Ref. 9.

E_2 (low)	A_1 (TO)	E_1 (TO)	E_2 (high)	A_1 (LO)	E_1 (LO)
102	379	410	439	574	591

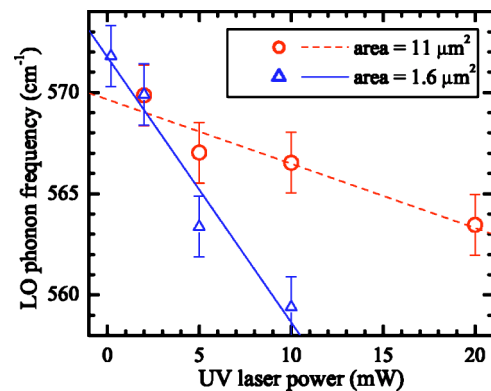


FIG. 3. (Color online). LO phonon frequency shift in ZnO quantum dots as a function of the excitation laser power. Laser wavelength is 325 nm. Circles and triangles correspond to the illuminated sample areas of $11\text{ }\mu\text{m}^2$ and $1.6\text{ }\mu\text{m}^2$.

The E_2 (high) peak in the spectrum of ZnO QDs is redshifted by 3 cm^{-1} from its position in the bulk ZnO spectrum (see Fig. 1). Since the diameter of the examined ZnO QDs is relatively large, such pronounced redshift of the E_2 (high) phonon peak can hardly be attributed only to the optical phonon confinement by the QD boundaries. Measuring the anti-Stokes spectrum and using the relationship between the temperature T and the relative intensity of Stokes and anti-Stokes peaks $I_S/I_{AS} \approx \exp[\hbar\omega/k_B T]$, we have estimated the temperature of the ZnO QD powder under visible excitation to be below $50\text{ }^\circ\text{C}$. Thus, heating in the nonresonant Raman spectra cannot be responsible for the observed frequency shift. Therefore, we conclude that the shift of E_2 (high) phonon mode is due to the presence of intrinsic defects in the ZnO QD samples, which have about 0.5% of impurities. This conclusion is supported by a recent study¹³ that showed a strong dependence of the E_2 (high) peak on the isotopic composition of ZnO.

Figures 2(a) and 2(b) show the measured resonant Raman scattering spectra of bulk ZnO and ZnO QDs, respectively. A number of LO multiphonon peaks are observed in both resonant Raman spectra. The frequency 574 cm^{-1} of 1LO phonon peak in bulk ZnO corresponds to A_1 (LO) phonon (see Table I), which can be observed only in the configuration when the *c*-axis of wurtzite ZnO is parallel to the sample face. When the *c*-axis is perpendicular to the sample face, the E_1 (LO) phonon is observed, instead.⁹ According to the theory of polar optical phonons in wurtzite nanocrystals,¹² the frequency of 1LO phonon mode in ZnO QDs should be between 574 and 591 cm^{-1} . However, Fig. 2(b) shows that this frequency is only 570 cm^{-1} . The observed redshift of the 1LO peak in the powder of ZnO QDs is too large to be caused by the intrinsic defects or impurities. The only possible explanation of the observed redshift is a local temperature raise induced by UV laser in the powder of ZnO QDs.¹⁴ To check this assumption, we varied the UV laser power as well as the area of the illuminated spot on the ZnO QD powder sample.

Figure 3 shows the LO phonon frequency in the powder of ZnO QDs as a function of UV laser power for two different areas of the illuminated spot. It is seen from Fig. 3, that for the illuminated $11\text{ }\mu\text{m}^2$ spot, the redshift of the LO peak increases almost linearly with UV laser power and reaches about 7 cm^{-1} for the excitation laser power of 20 mW. As expected, by reducing the area of the illuminated spot to

$1.6 \mu\text{m}^2$, we get a faster increase of the LO peak redshift with the laser power. In the latter case, the LO peak redshift reaches about 14 cm^{-1} for laser power of only 10 mW. An attempt to measure the LO phonon frequency using the illuminated spot of area $1.6 \mu\text{m}^2$ and UV laser power 20 mW resulted in the destruction of the ZnO QDs on the illuminated spot, which was confirmed by the absence of any ZnO signature peaks in the measured spectra at any laser power.

It is known that the melting point of ZnO powders is substantially lower than that of a ZnO crystal ($\sim 2000 \text{ }^\circ\text{C}$), what results in the ZnO powder evaporation at temperature less than $1400 \text{ }^\circ\text{C}$.¹⁵ The density of the examined ensemble of ZnO QDs is only about 8% of the density of ZnO crystal, which means that there is large amount of air between the QDs and, therefore, very small thermal conductivity of the illuminated spot. This explains the origin of such strong excitation laser heating effect on the Raman spectra of ZnO QDs.

If the temperature rise in our sample is proportional to the UV laser power, then the observed 14 cm^{-1} LO phonon redshift should correspond to a temperature rise around $700 \text{ }^\circ\text{C}$ at the sample spot of area $1.6 \mu\text{m}^2$ illuminated by the UV laser with power 10 mW. In this case the increase of the laser power to 20 mW would lead to the temperature of about $1400 \text{ }^\circ\text{C}$ and the observed destruction of the QD sample spot. To verify this conclusion we have calculated the LO phonon frequency of ZnO as a function of temperature. Taking into account the thermal expansion and anharmonic coupling effects, the LO phonon frequency can be written as¹⁶

$$\begin{aligned} \omega(T) = \exp \left\{ -\gamma \int_0^T [2\alpha_{\perp}(T') + \alpha_{\parallel}(T')] dT' \right\} \\ \times (\omega_0 - M_1 - M_2) + M_1 \left(1 + \frac{2}{e^{\hbar\omega_0/2k_B T} - 1} \right) \\ + M_2 \left(1 + \frac{3}{e^{\hbar\omega_0/3k_B T} - 1} + \frac{3}{(e^{\hbar\omega_0/3k_B T} - 1)^2} \right), \quad (1) \end{aligned}$$

where the Grüneisen parameter of the LO phonon in ZnO $\gamma=1.4$,¹⁷ the thermal expansion coefficients $\alpha_{\perp}(T)$ and $\alpha_{\parallel}(T)$ for ZnO are taken from Ref. 18, and the anharmonicity parameters M_1 and M_2 are assumed to be equal to those of the $A_1(\text{LO})$ phonon of GaN:¹⁶ $M_1=-4.14 \text{ cm}^{-1}$ and $M_2=-0.08 \text{ cm}^{-1}$. By fitting of the experimental data shown in Fig. 3 (area= $1.6 \mu\text{m}^2$) with Eq. (1), the LO phonon frequency at $T=0 \text{ K}$, ω_0 , was found to be 577 cm^{-1} . At the same time, it followed from Eq. (1) that the observed 14 cm^{-1} redshift shown in Fig. 3, indeed, corresponded to ZnO heated to the temperature of about $700 \text{ }^\circ\text{C}$.

In conclusion, we have clarified the origin of the phonon peak shifts in ZnO QDs. By using nonresonant and resonant

Raman spectroscopy, we have determined that there are three factors contributing to the observed peak shifts. They are the optical phonon confinement by the dot boundaries, the phonon localization by defects or impurities, and the laser-induced heating in nanostructure ensembles. While the first two factors were found to result in phonon peak shifts of few cm^{-1} , the third factor, laser-induced heating, could result in the resonant Raman peak redshift as large as tens of cm^{-1} . The obtained results shed new light on the controversial issue of the interpretation of Raman spectra of ZnO nanostructures and confirm theoretical model developed in Ref. 12. The recipes presented in this letter can be used to identify peaks in the Raman scattering spectra from ZnO nanostructures.

The authors acknowledge the financial and program support of the Microelectronics Advanced Research Corporation (MARCO) and its Focus Center on Functional Engineered Nano Architectonics (FENA).

¹X. T. Zhang, Y. C. Liu, Z. Z. Zhi, J. Y. Zhang, Y. M. Lu, D. Z. Shen, W. Xu, G. Z. Zhong, X. M. Fan, and X. G. Kong, *J. Phys. D* **34**, 3430 (2001).

²C. Bundesmann, N. Ashkenov, M. Schubert, D. Spemann, T. Butz, E. M. Kaidashev, M. Lorenz, and M. Grundmann, *Appl. Phys. Lett.* **83**, 1974 (2003).

³H. T. Ng, B. Chen, J. Li, J. Han, M. Meiyappan, J. Wu, S. X. Li, and E. E. Haller, *Appl. Phys. Lett.* **82**, 2023 (2003).

⁴X. Wang, Q. Li, Z. Liu, J. Zhang, Z. Liu, and R. Wang, *Appl. Phys. Lett.* **84**, 4941 (2004).

⁵Y. J. Xing, Z. H. Xi, Z. Q. Xue, X. D. Zhang, J. H. Song, R. M. Wang, J. Xu, Y. Song, S. L. Zhang, and D. P. Yu, *Appl. Phys. Lett.* **83**, 1689 (2003).

⁶M. Rajalakshmi, A. K. Arora, B. S. Bendre, and S. Mahamuni, *J. Appl. Phys.* **87**, 2445 (2000).

⁷H. Zhou, H. Alves, D. M. Hofmann, W. Kriegseis, B. K. Meyer, G. Kaczmarczyk, and A. Hoffmann, *Appl. Phys. Lett.* **80**, 210 (2002).

⁸Z. Wang, H. Zhang, L. Zhang, J. Yuan, S. Yan, and C. Wang, *Nanotechnology* **14**, 11 (2003).

⁹N. Ashkenov, B. N. Mbenkum, C. Bundesmann, V. Riede, M. Lorenz, D. Spemann, E. M. Kaidashev, A. Kasic, M. Schubert, M. Grundmann, G. Wagner, H. Neumann, V. Darakchieva, H. Arwin, and B. Monemar, *J. Appl. Phys.* **93**, 126 (2003).

¹⁰J. F. Scott, *Phys. Rev. B* **2**, 1209 (1970).

¹¹H. Richter, Z. P. Wang, and L. Ley, *Solid State Commun.* **39**, 625 (1981).

¹²V. A. Fonoberov and A. A. Balandin, *Phys. Rev. B* **70**, 233205 (2004); V. A. Fonoberov and A. A. Balandin, *Phys. Status Solidi C* **1**, 2650 (2004).

¹³J. Serrano, F. J. Manjon, A. H. Romero, F. Widulle, R. Lauck, and M. Cardona, *Phys. Rev. Lett.* **90**, 055510 (2003).

¹⁴L. Bergman, X. B. Chen, J. L. Morrison, J. Huso, and A. P. Purdy, *J. Appl. Phys.* **96**, 675 (2004).

¹⁵K. Park, J. S. Lee, M. Y. Sung, and S. Kim, *Jpn. J. Appl. Phys., Part 1* **41**, 7317 (2002).

¹⁶W. S. Li, Z. X. Shen, Z. C. Feng, and S. J. Chua, *J. Appl. Phys.* **87**, 3332 (2000).

¹⁷F. Decremps, J. Pellicer-Porres, A. M. Saitta, J. C. Chervin, and A. Polian, *Phys. Rev. B* **65**, 092101 (2002).

¹⁸H. Iwanaga, A. Kunishige, and S. Takeuchi, *J. Mater. Sci.* **35**, 2451 (2000).